THE 89-ENERGY GROUP NEUTRON SPECTRA FOR THE MK4 AND MK7 FAST NEUTRON ROD MATERIAL TESTING FACILITIES IN NRU

T.C. Leung & L. Walters
AECL Chalk River Laboratories, Chalk River
Ontario, CANADA KOJ 1J0
leungt@aecl.ca watersl@aecl.ca

Abstract

The NRU reactor at Chalk River provides two types of fast neutron rods (Mark 4 and Mark 7) as irradiation facilities to study the effects of fast neutrons (E> 1 MeV) on zirconium reactor materials for assessing material damage and deformation. There is a need to extend the material testing to Inconel materials which are sensitive to lower neutron energies. This paper describes the 89-group neutron spectra in the two Fast Neutron Rods in NRU, comparisons with the spectra in typical CANDU reactors, and the use of the two spectra for spectral effect predictions on material behavior.

1. Introduction

The National Research Universal (NRU) reactor at Chalk River began operation in 1957. It is used to carry out research in basic science and in support of the CANDU power reactor programs, such as the fuel bundle and material development programs. It is also a major supplier of medical radioisotopes in Canada and the world. The NRU reactor is heavy water cooled and moderated, with on-line refueling capability. It is licensed to operate at a maximum power of 135 MW, and has a peak thermal flux of approximately 4.0×10^{18} $n.m^{-2}.s^{-1}$. Figure 1 shows an NRU core lattice, with 31 rows and 18 columns (A to S, with no column "I"). The hexagonal lattice pitch is 19.685 cm.

The NRU reactor provides two types of fast neutron rods to study the effects of fast neutron irradiation of reactor materials. Materials of specific interest are zirconium and its alloys, which are used in the pressure tubes and calandria tubes of CANDU reactors. Various in-reactor material test programs have been conducted in NRU for many years, including experiments on irradiation-induced creep and growth, on corrosion and on fracture properties. In general, displacement of atoms due to irradiation can occur by a variety of processes. The two main processes that apply to materials in the core of a power reactor are (i) atom displacement and cascade from direct neutron collisions (ii) thermal neutron capture and subsequent gamma, proton and alpha particle release coupled with atomic recoil. The displacement damage that affects the in-core zirconium alloy material properties is caused primarily by direct neutron collisions.

Between 2009 May and 2010 August, the NRU reactor was shut down 15 months for vessel repair, and since restart it has operated safely and reliably. At present, the AECL Nuclear Laboratories are seeking new opportunities for material testing and research in NRU from universities and industry. Recently, a need was identified for the testing of materials which are also sensitive to the lower energy portion of the neutron spectrum.

The Inconel X-750 components in the CANDU reactor contain ~70% Ni and are distinct in that absorption of thermal neutrons by the most abundant isotope Ni-58 produces Ni-59, which has three highly exothermic reactions: (n,α), (n,γ), (n,p). These reactions contribute to displacement damage and the generation of significant amounts of helium and hydrogen. Experimental investigations into the effects of irradiation damage on this material will be performed in the NRU reactor.

This paper describes the 89-energy neutron spectra for the two types of fast neutron rod (Mark 4 and Mark 7) materials testing facilities in the NRU reactor. Comparisons of the spectra with those in typical CANDU reactors are given. The use of the two neutron spectra for material testing predictions is then briefly described.

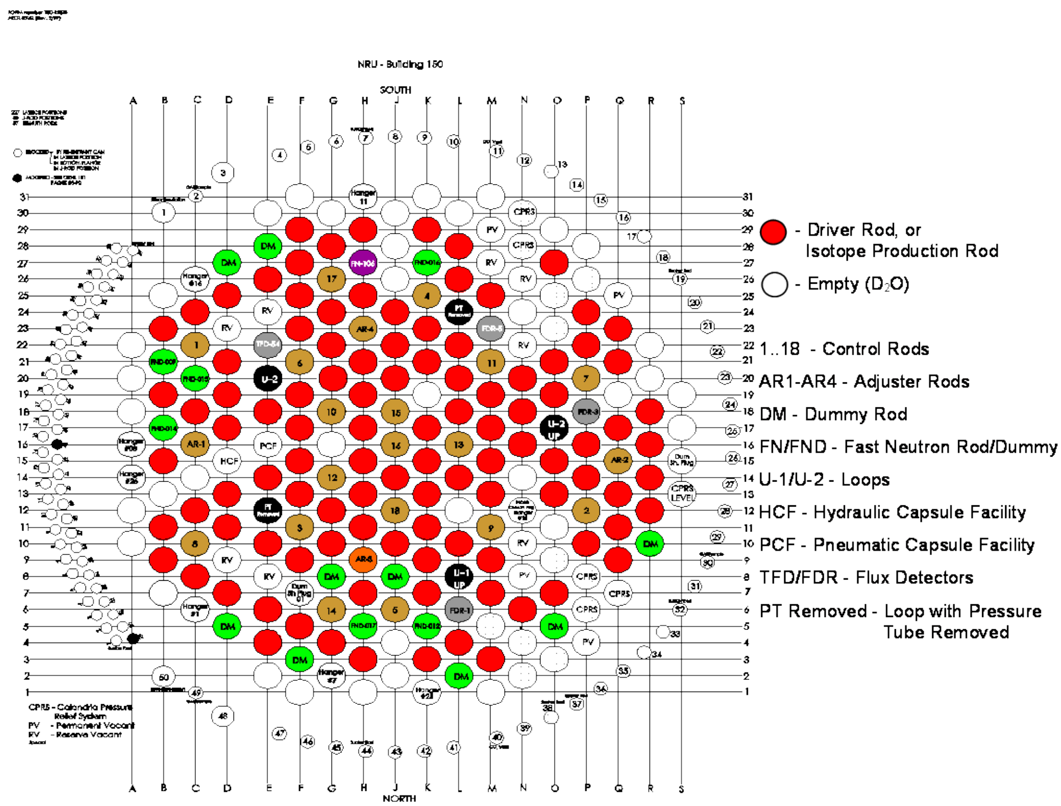

Figure 1 The NRU Core Lattice

2. Materials Testing in Fast Neutron Rods

2.1 Mark 4 Fast Neutron Rods

Figure 2 shows a Mark 4 Fast Neutron (Mk4 FN) rod, which has an overall length of 7.825 metres. It consists of an outer flow tube and an inner flow tube with its bottom end closed to form a cavity. Experimental inserts enclosed in pressure tubes are placed inside the central cavity. At the top of each experimental insert is an integral shielding plug, with tubes for the passage of service leads and water piping for cooling.

A Mk4 rod contains approximately 32 kg of natural uranium, in the form of sintered UO_2 fuel arranged in three 15-element bundles, each approximately 49.5 cm long. The fuel pins are located in the annulus formed by outer and inner flow tubes, and are cooled by heavy water. The maximum operating power for a Mk4 FN rod is 1.65 MW.

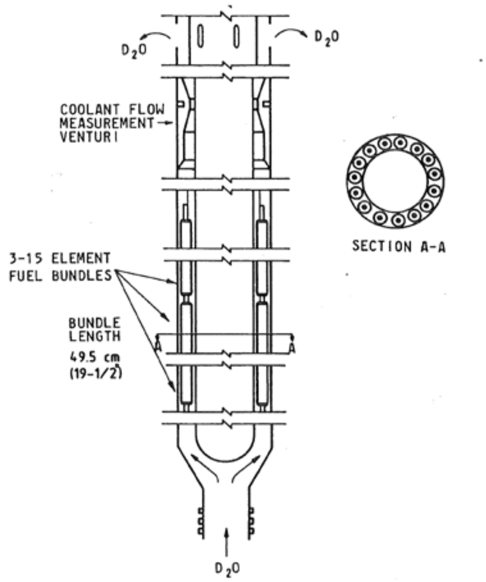

Figure 2 The Mk4 FN Rod.

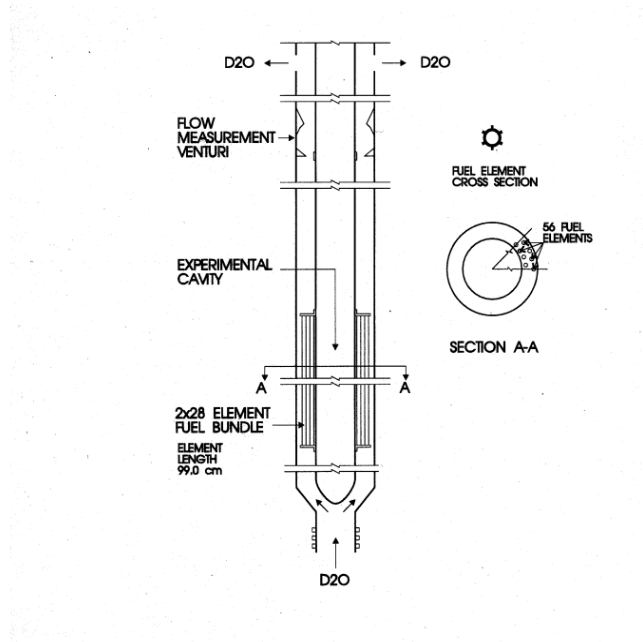

Figure 3 The Mk7 FN Rod

2.2 Mark 7 Fast Neutron Rods

Figure 3 shows a Mark 7 Fast Neutron (Mk7 FN) rod, which has an overall length of 7.822 m. It consists of an outer flow tube and an inner flow tube with bottom-end closed to form a cavity. The experimental inserts are enclosed in a pressure tube and placed inside this cavity. To cool specimens in the pressure tube, the coolant flows down through a central flow tube and upward to cool the specimens.

The fuel for the Mk 7 FN rod is made up of 56 elements, arranged in two rings of 28, containing low enriched uranium (LEU) fuel, the same as the fuel in an NRU driver rod. The LEU fuel alloy is dispersion-type Al-61.4 wt% U_3Si, consisting of particles of U_3Si dispersed in a continuous aluminum matrix, with 19.75 % U-235 in uranium. Each fuel element is 99.06 cm long, with a fuel length of 81.28 cm, located at the mid-height of the reactor. The fuel provides a uniform axial fast neutron flux region approximately 60 cm in length inside the experimental cavity. The Mk 7 FN rod is designed to operate, with an experimental insert, at a maximum power of 2.64 MW to the coolant.

3. Method of Calculation of the 89-Group Neutron Spectra

Calculations of the fast-neutron flux spectra in the experimental cavities of the Mk7 and Mk4 FN rods were performed using the WIMS-AECL code [1,2], with its associated ENDF/B-V derived data base. WIMS-AECL is a multi-group transport code with two-dimensional capabilities using the “Pij” collision probability method. The main transport calculations were performed using 89 energy groups.

The experimental section of the material testing facility was modeled as a super-cell, which included the cell-of-interest and a representation of its environment. The neighbouring fuel rods provide the correct driving spectrum for the FN rod, and are modeled as two fuel rings located at radii of 20.2 cm and 39.9 cm from the centre of the cell. The fuel loading in these two rings was about 2.39 g/cm and 4.34 g/cm of U-235. A adjustable boron-10 ring was added outside the fuel rings, in order to keep the k-effective close to 1.000 throughout the burnup range.

The experimental insert was modeled as four annuli: the first for the centre flow tube, the second for the inner support tube, the third for the specimen holder and specimens, and the fourth for the enclosing pressure tube. The radii and material composition of the third annulus varied slightly, depending on which type of specimen holder assembly was used.

For the neutron spectrum calculation, the version of WIMS-AECL used was version 2.5d, and the older data library of ENDFB/V was used, so that the calculation method was the same as with the rest of the NRU assemblies. In the future the neutron spectra could be re-calculated using a newer version of WIMS-AECL, such as 3.1, and different data libraries, ENDFB/VI or /VII. It is expected that variation of the calculated neutron spectra using different version of WIMS-AECL and different data libraries would be small.

4. Results of Neutron Spectra Calculations

4.1 Mk7 and Mk4 Rod Neutron Spectra

A reference case was set up to model a typical Mk7 rod, with a zirconium pressure tube thickness of 3.5 mm, and a 3.0 mm gap between the pressure tube and the inner flow tube of the rod. The rod was assumed to be fresh with no fuel burnup. Column 3 of Table 1 lists the WIMS calculated neutron fluxes at the specimen irradiation location inside the experimental cavity of the NRU Mk7 FN rod for the reference case. Because some reactor materials, such as the Inconel garter spring, will experience damage from both fast and thermal neutrons (see Sec. 4.3), Table 1 lists details of the neutron spectrum for both the fast energy groups (E>1MeV) and the thermal energy groups below 0.0625 eV. The neutron fluxes are normalized to the rod design power of 2.64 MW to the coolant.

Table 1 Comparison of Fast and Thermal Neutron Spectra inside the Experimental Cavities of a Mk 7 Rod and a Mk 4 Rod.

Group	**Energy Width (MeV)**	**Mk 7 Rod Flux ($\times 10^{16} n.m^{-2}.s^{-1}$)**	**Mk 7 Rod Flux (% of total)**	**Mk 4 Rod Flux ($\times 10^{16} n.m^{-2}.s^{-1}$)**	**Mk 4 Rod Flux (% of total)**
1	7.79-10.0	0.573	0.110	0.176	0.055
2	6.07-7.79	1.593	0.307	0.500	0.157
3	4.72-6.07	3.584	0.690	1.114	0.350
4	3.68-4.72	6.007	1.156	1.814	0.570
5	2.87-3.68	8.926	1.718	2.713	0.853
6	2.23-2.87	11.633	2.239	3.580	1.125
7	1.74-2.23	11.743	2.260	3.469	1.091
8	1.35-1.74	12.259	2.359	3.676	1.156
9	1.05-1.35	11.728	2.257	3.541	1.113
Fast E>1.05MeV	Sub-total	68.045	13.094	20.584	6.471
Epi-thermal	0.625×10^{-6} -1.05	245.957	47.329	90.266	28.377
66	$(0.5\text{-}0.625)\times10^{-6}$	1.367	0.430	2.735	0.526
67	$(0.4\text{-}0.5)\times10^{-6}$	1.414	0.444	2.779	0.535
68	$(0.35\text{-}0.4)\times10^{-6}$	0.880	0.277	1.693	0.326
69	$(0.32\text{-}0.35)\times10^{-6}$	0.616	0.194	1.158	0.223
70	$(0.3\text{-}0.32)\times10^{-6}$	0.467	0.147	0.856	0.165
71	$(0.28\text{-}0.3)\times10^{-6}$	0.539	0.169	0.956	0.184
72	$(0.25\text{-}0.28)\times10^{-6}$	0.998	0.314	1.664	0.320
73	$(0.22\text{-}0.25)\times10^{-6}$	1.412	0.444	2.124	0.409
74	$(0.18\text{-}0.22)\times10^{-6}$	3.348	1.052	4.352	0.837
75	$(0.14\text{-}0.18)\times10^{-6}$	7.859	2.471	8.807	1.695
76	$(0.10\text{-}0.14)\times10^{-6}$	20.216	6.355	20.596	3.963
77	$(0.08\text{-}0.10)\times10^{-6}$	19.289	3.712	19.696	6.192
78	$(0.067\text{-}0.08)\times10^{-6}$	17.311	3.331	18.014	5.663
79	$(0.058\text{-}0.067)\times10^{-6}$	14.570	2.804	15.322	4.817
80	$(0.05\text{-}0.058)\times10^{-6}$	14.804	2.849	15.695	4.934
81	$(0.042\text{-}0.05)\times10^{-6}$	16.429	3.161	17.532	5.512
82	$(0.035\text{-}0.042)\times10^{-6}$	15.429	2.969	16.565	5.208
83	$(0.030\text{-}0.035)\times10^{-6}$	11.352	2.184	12.244	3.849
84	$(0.025\text{-}0.03)\times10^{-6}$	11.317	2.178	12.249	3.851
85	$(0.02\text{-}0.025)\times10^{-6}$	10.907	2.099	11.844	3.723
86	$(0.015\text{-}0.02)\times10^{-6}$	9.986	1.922	10.874	3.419
87	$(0.01\text{-}0.015)\times10^{-6}$	8.391	1.615	9.160	2.880
88	$(0.005\text{-}0.01)\times10^{-6}$	5.899	1.135	6.448	2.027
89	$(0.002\text{-}0.005)\times10^{-6}$	2.269	0.437	2.480	0.780
Thermal	Below 0.625×10^{-6}	205.672	39.577	207.238	65.151
Total		519.674	100.00	318.090	100.00

The operating flux and power of the Mk7 rod in an NRU core configuration can be calculated using the TRIAD code [3]. For the LEU fuel used in the Mk7 rod, the fuel power-to-coolant ratio was taken to be 0.94, and the fission power from the Mk7 rod is (2.64/0.94)=2.81 MW. For a fuel length of 81.28 cm, the linear fission power of the rod is 3.45 MW/m. In column 3 of Table 1, the fast neutron flux above 1 MeV at the specimen irradiation location is 6.8 x 10^{17} $n.m^{-2}.s^{-1}$, the thermal neutron flux below 0.625 eV at the same location is 2.06 x 10^{18} $n.m^{-2}.s^{-1}$, and the total neutron flux is 5.20 x 10^{18} $n.m^{-2}.s^{-1}$. In percentages, the fast neutron flux above 1 MeV is 13.1% of the total, and the thermal flux is 39.6%.

Similar flux spectrum calculations were performed for the NRU Mk4 FN rod, and the results are listed in columns 5 and 6 of Table 1. The neutron flux is normalized to a linear rod power of 1.05 MW/m, or 1.65 MW total rod power. The Mk4 FN rod produces less than one third of the fast neutron flux of the Mk7 rod (2.06 vs 6.80 x $10^{17}$$n.m^{-2}.s^{-1}$). Also, for the NRU Mk4 FN rod, the percentage of fast neutron flux above 1 MeV is only 6.5% of the total, and the thermal flux is 65.2%.

4.2 Comparison of Mk4 and Mk7 Rod Neutron Spectra with CANDU Reactor

Figure 4 shows that the neutron spectra in the fast neutron rods are similar to the spectra in the CANDU pressure tube locations. Each neutron spectrum is normalized to its own total fluxes, for example, 5.19, 3.18, and 4.59 x10^{14} $n.cm^{-2}.s^{-1}$for the Mk7, Mk4 and CANDU total fluxes, respectively. The CANDU fluxes were also calculated using WIMS-AECL, version 2.5d. In assessing the total material damage, it needs the total fluxes for the whole energy spectrum.

In the thermal neutron energy range in Figure 4, the CANDU fluxes are slightly higher than the Mk7 and Mk4 rod fluxes, while in the fast neutron energy range, the CANDU fluxes fall between the other two. This makes these facilities ideal locations to irradiate materials which are sensitive to the effects of neutron spectra as they will induce similar levels of radiation damage and gas production that the material would experience during service in a CANDU reactor. It is also noted in this Figure that Mk7 and MK4 fluxes show the same magnitude in low energy, but Table 1 show 65% for Mk4 and only 40% for Mk7, because Mk7 has a higher total flux than that of Mk4.

The total flux in NRU is lower than in many other material test reactors (MTRs) outside Canada, which means that NRU is not optimum for end-of-life materials studies; however, a low flux is ideal to study stress relaxation and transient phenomena where the majority of the changes to the material are occurring over relatively low doses (~1x10^{25} $n.m^{-2}$). Also, since the flux levels are similar to CANDU, performing materials irradiation tests in NRU rather than in a high flux MTR eliminates the possibility of introducing different rate-dependent changes in point defect concentrations and their effects on vacancy-interstitial recombination rates.

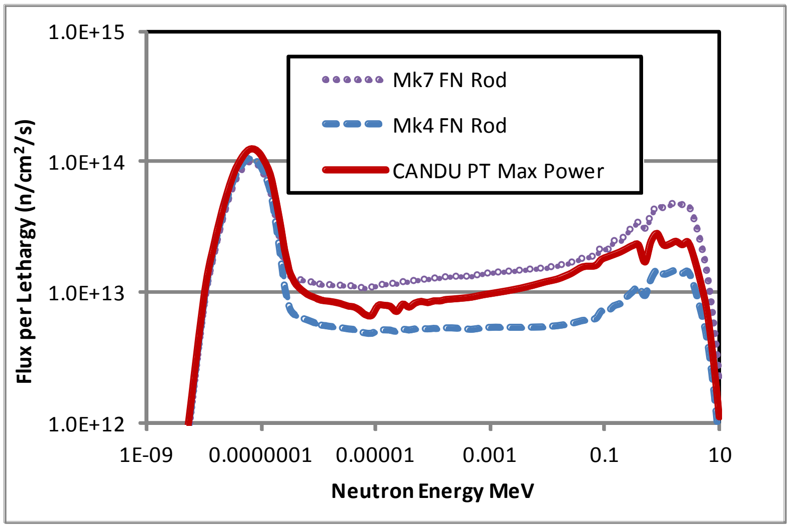

Figure 4. Flux per lethargy vs Neutron energy

4.3 Use of Mk4 and Mk7 Rod Neutron Spectra for Material Test Predictions

In the core of a nuclear reactor, most of the atomic displacement damage that gives rise to enhanced creep is caused primarily by direct collisions of fast neutrons with atoms in the components. The damage process follows several stages. In a single crystal of zirconium, the displacement energy of the crystal lattice needs a threshold energy of an incoming neutron to cause damage. A zirconium atom is about ninety times the mass of a neutron. Thus, if the primary knock-on (PKA) zirconium atom is bound to the lattice by 40 eV, the minimum energy of a neutron that can cause displacement by a direct collision must be ~1 keV. Neutron energies below this threshold cannot displace zirconium nuclei from lattice positions and hence no mobile zirconium interstitials are created.

If the neutron energy is above the threshold displacement energy, the recoil energy of the PKA is transferred to nearby zirconium nuclei. The PKA is charged and thus partially slowed by electrical repulsion leading to heat. However, much of its energy is transferred by direct collision to nearby zirconium nuclei which, in turn, recoil and are displaced from their lattice positions. Each is able to participate in secondary collisions. A collision cascade develops that can involve hundreds of displaced atoms, the number depending on the initial PKA recoil energy. This cascade happens in a very short time. Once the cascade forms, the internal electrical forces amongst defects and the temperature dependence of interstitial diffusion cause most of the mobile interstitials to recombine at a nearby lattice vacancy. It is estimated that up to 10% of the displaced atoms never find their way back to a lattice position.

The current method for determining radiation damage is to obtain calculated neutron spectrum data and then compute the relative damage rates using compatible damage cross sections. The cross sections describe the relative probability of causing an atomic displacement. Therefore, the chance of a nuclear reaction is described by a set of multigroup fluxes (φ_g in n/cm^2/s) combined with a set of energy-dependent neutron damage cross sections (σ_g in eV-cm^2). The damage rate, R, in eV/s for an atom density of (Σ_g in cm^{-1}), is computed as:

$R = \Sigma_g \, \varphi_g \, \sigma_g$ where the sum is over all energy groups, $_g$.

The damage cascade caused by a head-on collision between a zirconium nucleus and a fast neutron of incident energy 1 MeV may contain up to 400 displaced atoms. Multiplying the damage rate R by 0.8/(2*40) gives the displacement rate dpa/s [4,5]. Figure 5 shows a comparison of the dpa generated in Zr-2.5Nb CANDU pressure tube materials using the spectra shown in Figure 4.

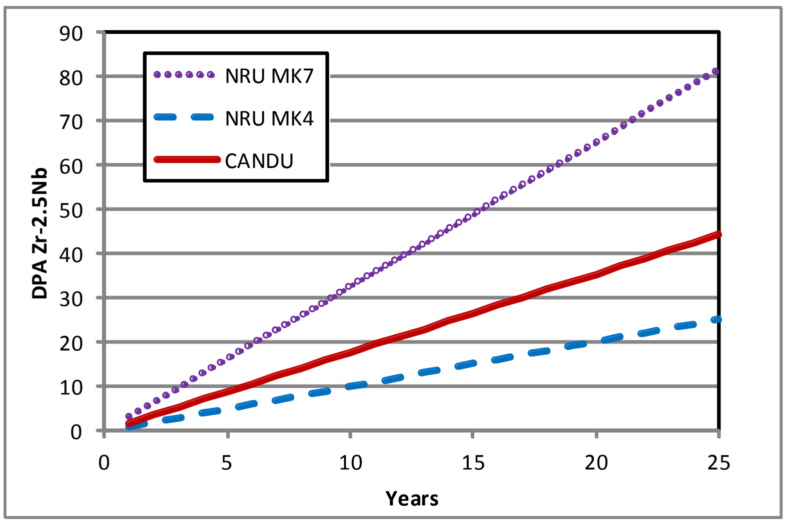

Figure 5. DPA for Zr-2.5Nb Material in NRU FN Rods and in a Maximum Power CANDU Pressure Tube

Using dpa from fast neutrons is valid for comparison of data from various spectral environments only if no other process is acting strongly. Displacements caused by thermal neutrons in a CANDU reactor core can usually be neglected, especially for zirconium components. However, for components containing natural nickel neutron absorption at thermal energies will cause the following transmutations.

$$\begin{aligned}
&\text{Ni-58} + n \rightarrow \text{Ni-59} + \gamma \\
&\text{Ni-59} + n \rightarrow \text{Fe-56} + \text{He-4} \\
&\text{Ni-59} + n \rightarrow \text{Co-59} + \text{H} \\
&\text{Ni-59} + n \rightarrow \text{Ni-60} + \gamma
\end{aligned}$$

Therefore, Inconel garter springs (which contain ~70% Ni) will experience damage from all energies including fast neutrons (E> 0.1MeV) and thermal neutrons (E<0.5 eV).

Transmutation of Ni-58 to N-59 with subsequent (n,p) and (n, α) processes produces a significant additional component to the total damage. Although the ejected particles cause displacements, by far the biggest contribution to the displacement per event is the atom recoil. Details of the damage production for the (n,α), (n,p) and (n,γ) reactions are given in [6,7]. In calculations, the displacements due to the recoil and those caused by the ejected particle are factored in for the (n,α) and (n,p) reactions. Only the recoil effect is factored into the damage production for the (n,γ) reaction.

For Ni-58, the minimum neutron energy needed to cause direct displacement damage is 580 eV when the atomic displacement threshold energy is 40 eV. The isotope Ni-59 has relatively high thermal neutron capture cross section which enables the production of helium and hydrogen [6,7]. Since Ni-59 does not exist in natural nickel, it is only generated from the thermal neutron capture reaction. For the (n,α) reaction with Ni-59 the total damage energy is 176.2 keV per neutron capture and therefore the subsequent total number of displacements per neutron capture in Ni-59 is 1762 [6]. In a CANDU reactor at the garter spring location the dpa from the production of He-4 is larger than from fast neutron damage, as shown in Table 2.

Figures 6 and 7 show results for helium generation and dpa for Inconel X-750 material at the garter spring position in CANDU and in the FN rods. The calculations are based on the reaction described above only. By leaving out the contributions from high energy interactions with Ni and other alloying elements in X-750 such as Cr and Fe, the helium generation and dpa are under-predicted by ~5%, as compared to the calculations performed using the SPECTER code [8].

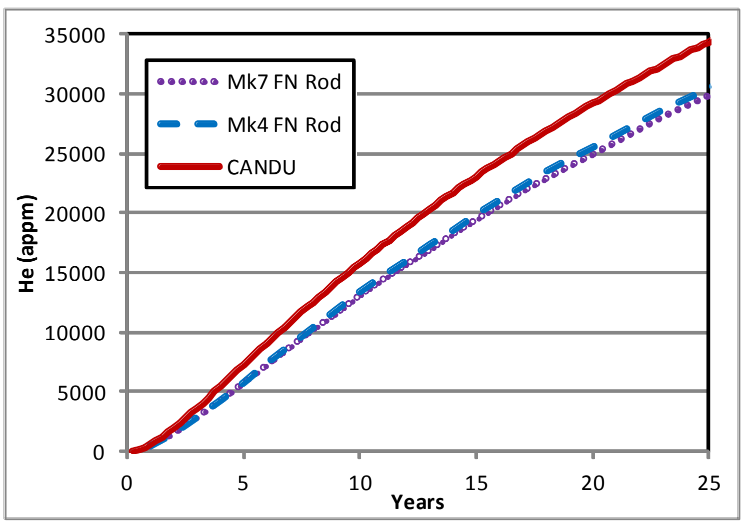

Figure 6. Helium Generated in Inconel X-750 Material in the NRU FN Rods and at the CANDU Garter Spring Location.

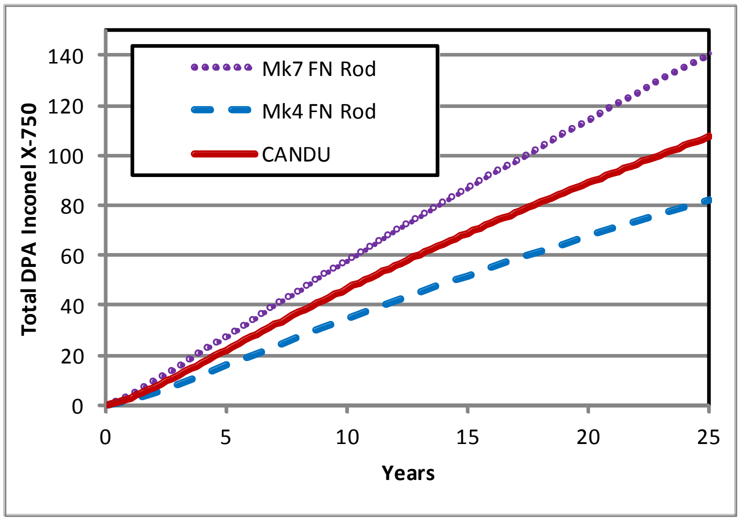

Figure 7. DPA in Inconel X-750 Material in the NRU FN Rods and at the CANDU Garter Spring Location.

Table 2 summarizes displacement rates for Zr-2.5Nb and X-750 materials in NRU fast neutron rods and in CANDU. Compared to the Mk4 rod, irradiation of zirconium alloy pressure tube material in a Mk7 rod is a quicker way to achieve the equivalent total damage. For in-reactor components containing natural nickel not only is there a contribution to displacements caused by atom recoil associated with photon emission, but more significantly the process of transmutation giving Ni-59 is a major contributor to the damage process.

Table 2. DPA Rates for Zr-2.5Nb and X-750 Test Materials in NRU fast neutron Rods and a Maximum Power CANDU Channel

	Mk7 FN Rod	Mk4 FN Rod	CANDU
dpa/yr from direct displacement in X-750 material	3.41	1.05	1.77
dpa /yr from (n,α) in X-750	2.0	2.04	2.27
dpa /yr from (n,p) in X-750	0.04	0.04	0.04
dpa /yr from (n,γ) in X-750	0.06	0.04	0.05
dpa /yr from direct displacement in Zr-2.5Nb material	3.27	1.01	1.77

5. Conclusions

Several conclusions can be drawn from the specific features of the two NRU fast neutron material testing facilities:

1) AECL Nuclear Laboratories can provide opportunities for material testing in the two NRU fast neutron irradiation facilities for universities and industry. Materials tests are not limited to damage due to fast neutrons, but also include materials tests that are sensitive to the thermal neutrons.
2) The 89-energy group energy spectra for the Mk7 and Mk4 rods were calculated using WIMS-AECL code, and the overall energy spectra are similar to those of the CANDU reactors. In the thermal neutron energy range, the CANDU fluxes are slightly higher than the Mk7 and Mk4 rod fluxes, while in the fast neutron energy range, the CANDU fluxes fall between the other two.
3) Based on the calculated 89-group energy spectra, materials test predictions in the NRU Mk7 and Mk4 rods, such as helium production, gamma and proton reaction rates, can be performed. Materials test results from NRU will be directly applicable in determining materials behavior in CANDU reactors.

6. Acknowledgements

The authors would like to thank R. Donders, S. Douglas and M. Griffiths from AECL and L. R. Greenwood from Pacific Northwest National Laboratory for their guidance and assistance with the assessment of spectral effects on material behavior.

7. References

[1] J.D. Irish and S.R. Douglas, "Validation of WIMS-IST", Proceedings of the 23rd Annual Conference of the Canadian Nuclear Society, Toronto, Canada, 2002 June.

[2] S.R. Douglas, "A calculational model for the NRU reactor", Paper presented at the Canadian Nuclear Society 1985 Annual Conference; also AECL Report, AECL-8841, 1985 June.

[3] T.C. Leung and M.D. Atfield, "Validation of the TRIAD3 Code Used for the Neutronic Simulation of the NRU Reactor", Proceedings of the 30th Annual Conference of the Canadian Nuclear Society, Calgary, Alberta, Canada, 2009 May 31 - June 3.

[4] D.G. Doran and N.J. Graves, "Neutron Displacement Damage Cross Sections for Structural Metals", ASTM STP 611 (1976), pp. 564-482.

[5] M.J. Norgett, M.T. Robinson, I.M. Torrens, "A Proposed Method of Calculating Displacement Dose Rates", Nuclear Engineering and Design 33 (1975), pp. 50-54.

[6] L.R. Greenwood, "A new calculation of Thermal Neutron Damage and Helium Production in Nickel", Journal of Nuclear Materials 115 (1983), pp. 137-142.

[7] L.R. Greenwood and F.A. Garner, “Hydrogen Generation arising from the ^{59}Ni(n,p) Reaction and its impact on Fission-Fussion Correlations”, Journal of Nuclear Materials 233-237 Part 2 (1996), pp. 1530-1534.

[8] L.R. Greenwood and R.K. Smither, “SPECTER: Neutron Damage Calculations for Materials Irradiations”, ANL/FPP/TM-197, Argonne National Laboratory, 1985.